XPAD : an hybrid pixel detector for material sciences studies using X-ray synchrotron radiation.

J.-F. Bérar, S. Arnaud, S. Basolo, N. Boudet, P. Breugnon, B. Caillot, J.-C. Clemens, P. Delpierre, B. Dinkespiler, S. Hustache, I. Koudobine, M. Menouni, P. Pangaud, R. Potheau, E. Vigeolas

D2AM/CRG-ESRF Grenoble — LdC-CNRS — SOLEIL St Aubin — CPPM-IN2P3-CNRS Marseille

Feb. 17th, 2006 — **Campinas sincrotron**

Summary.

Detectors & material sciences scattering

Imaging : → X-ray microscopy, X-ray topography, X-ray radiography
Spectroscopy : chemical composition (XAS), short order range (EXAFS)
Scattering by beam → $I(Q) \propto F^2(\rho_e)$

Intensity range in scattering experiments

$1 \rightarrow 10^4$	13b	mean structure	chemistry (biocrystallography)
$1 \rightarrow 10^6$	20b	ordering	correlation, incomensurate
$1 \rightarrow 10^9$	30b	SAXS	μm objects interaction, polymers

- Synchrotron → current flux on sample : $10^{11} - 10^{14}\ \nu/s$
- Spot size at sample or detector position : $1 \times 5 \rightarrow 0.05 \times 0.10\ mm^2$
- Counting rate : $10^9 \nu/s$ within $10^{-2} mm^2$
- Resolution : angular $10^{-3\,o} \rightarrow 100\,\mu m$ at $0.5\,m \approx 0.01^o$

On D2AM-CRG/ESRF beamline (BM2).

Very demanding experiments use slits and photomultipliers to reach the required quality.

In structural works, CCD cameras with indirect photon detection are commonly used.

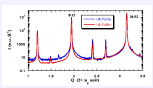

Diffuse scattering in icosaedral quasi-crystals : 7 orders of magnitude are necessary to measure this signal. Dynamic extended by **attenuators**, time consuming mapping

Complex shape of the diffusion around Bragg peak obtained by adding 10 (1000) frames. Out of peak to avoid blooming effects

Data from M. de Boissieu, see Phil. Mag. Let. (2001) 81, 273-283 and (2003) 83, 1-29

D2AM-CRG/ESRF detector requirement

dynamic range	$> 10^8 count/pixel$	⇒ 32 bits architecture
saturation rate	$> 10^7 \nu/s/pixel$	⇒ noise $< 0.1\,\nu/s/pixel$
energy range	$5 \rightarrow 25\,keV$	from beamline
pixel size	$250 \times 400\,\mu m^2$	mean spot size in 1995
exposure time	$1ms \rightarrow 1000\,s$	kinetics potentiality

High energy physics experiments lead to built detector like Delphi at CERN which uses the potentiabilities offered by microelectronics and direct photon conversion in silicon.

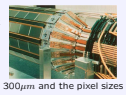

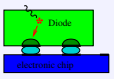

The silicium thickness $300\mu m$ and the pixel sizes $330 \times 330\mu m^2$ were convenient to our beamline requirements leading to the project of buildind a new X-ray detector taking benefit of the Delphi detector peoples knowledge.

The XPAD project (XPAD1).

- Absorbed photons
→ electron clouds
→ charge migration
→ electron bunches
→ pixel threshold
→ pixel counters
→ on-board memories
→ ethernet data

Diodes :
- high resistivity Si

Chips :
- AMS CMOS $0.8\,\mu m$
- 24×25 pixel/chip

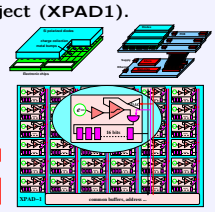

Boudet et all., NIM A510 (2003) 41-44. Berar et all., J. Appl. Cryst. 35 (2002) 471-476

XPAD detectors.

	XPAD1 2001	XPAD2 2003	XPAD3 2006
pixel size	$330 \times 330\ \mu m$		$130 \times 130 \mu m$
foundry	AMS $0.8\ \mu m$ CMOS		IBM $0.25 \mu m$
pixel / chips	24×25 pixels		80×120 pixels
internal counters	16 bits		14 bits
overflow counters	16 bits		16 bits
energy range	15 to 25 keV		7 to 25 keV
sensor	Si $300\ \mu m$ (Delphi)		Si $500\ \mu m$
counting rate	$1.10^6 ph/s$		$2.10^6 ph/s$
time constant	500 ns with detector	208 ns with detector	*to be measured*
modules	5×2 chips	8×1 or 8×8 chips	8×7 chips
detector	1 module	up to 8 modules	
electronic	reduced	back plugged	
connection	parallel wires	ethernet 100MB	

XPAD2 detector : 8 modules × 8chips

New diodes of $500\mu m$ Si thick → efficiency 78 % @15keV, 21% @25keV

Diode = 8 chips of 24×25 pixels
PCB card : drivers and regulators.
Modules = acquisition card
Alterra Nios kit + ethernet

Tiled as close as possible → reduce shading, dead zones.
Metallic holder → few μm.
Size : 200×192 pixels
Surface $\approx 68 \times 68 mm^2$.

Interface software developed using LabWindows/CVI application software moves to Linux.
XPAD prototype at SAXS station.

Dead area in pixel detectors

The mechanical structure of such detector induces some dead area, it seems necessary to minimize it or at less to know it.

Within modules : No dead area Pixels at the border of the chip are connected to pixel diode with an increased surface to avoid dead area associated with the packing of chips on the detector : mechanical border, guards ring...
Between modules : ≈ 1 pixel/column ⇒ 4% XPAD2 → 1% XPAD3

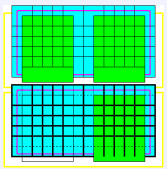

Spatial resolution

As the diode is common to pixels belonging to the same chip, some charge sharing may occurs between adjacent pixels. Measurements show that the charge sharing occurs on ≈ $60\,\mu m$.

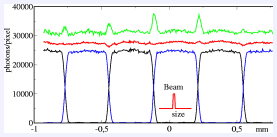

A flat field can be obtained when energies edge is perfectly adjusted in each pixel (red). In case of too low edges, this share sharing create some over-counting at pixel borders (green).

Dynamical range

Counts in adjacent pixels as a function of the incoming flux.

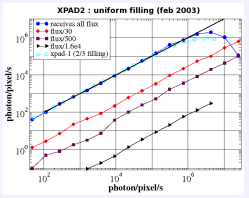

No blooming effect

- Overall dead time ≈ 0.21μs
- Xpad chip dead time < 0.10μs

Dynamical range (XPAD1 application)

Diffusion (left) of a CdYb icosahedral quasicrystal and associated rotation image (right) on which the highest peak is near counter saturation rate, it cross the Ewald sphere within a few part of the exposure!

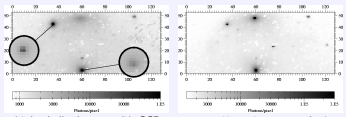

To obtain similar images with CCD cameras : attenuator are required and a few hundred images have to be summed.

Energy resolution

The conversion of incoming photons in silicon leads to a charge proportional to the incoming energy. The XPAD chip energy resolution is near $1\,keV$.

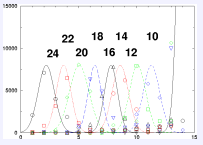

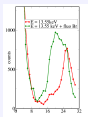

Measured counts as a function of the threshold for the diffusion of a Br solution on both sides of Br absoption edge.

Pixel threshold register : 4 bits (XPAD1) → 6 bits (XPAD2)

XPAD2 calibration and dispersion (1)

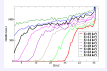

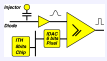

- *beam* E_x : monochromatic flat scattering (amorphous), noisy, time expensive
- *injection* E_{inj} : simulate the beam, quick and easy but need calibration
- Each pixel is described by : $C, \alpha, \beta, E_{inj}(noise)$
$E_x = CE_{inj} = \alpha(I_{th}) + \beta(I_{dac})$
$E_x(noise) = CE_{inj}(noise)$
- ≈ $4\,10^4$ pixels ⇒ automatic configuration/calibration procedure.

Knowing these characteristics :
the setup of each chip at a given energy E can be defined as the value of the chip common threshold level I_{th} for which most of the pixels can be fine tune, $I_{dac} \in [0, 63]$.

XPAD2 calibration and dispersion (2)

- XPAD2 initial threshold dispersion $60\,e^-$
⇒ pixels not tuned < 3%
- manufacturing problems :
leakage in bumping process
⇒ new foundry using the same masks
- threshold dispersion increase strongly
≈ $120\,e^-$ on most chips
⇒ pixels not tuned < 15%

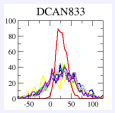

However, even if all the pixels are not perfectly set, the XPAD2 detector appears as a usefull tool for recording new data in SAXS and diffraction on a synchrotron beamline in the range 15 - 25 keV.

SAXS application (1)

Scattering of some samples recorded at BM2-SAXS camera using XPAD detector at $20\,keV$.

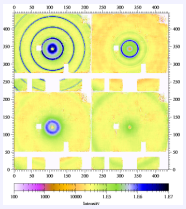

- Ag Behenate
- Bee waxs
- Polyurethan
- Empty cell
- Teflon
- Water (5mm)

SAXS application (2)

Data have been compared with FOB CCD* ones using the same setting.

The low noise achieved with the XPAD detector allows to improve the measurement of weak scatterer like water : the signal observed without sample is really lower with XPAD than with the CCD (fluorescence, PSF tails ...)

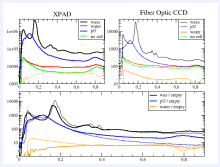

* PI-SCX-1300, Roper Scientific (EEG 1340x1300, 50μm pixel size, dark corrected)

Powder diffraction application (1)

Scintillator and slits → 2d-detector.
- Diffraction along cones
- Data redondancy with 2D detector
- 60° collected at high resolution
- angular aperture 4^o at $1m$

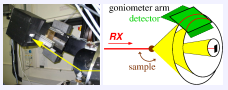

With 0-D detector pipes and slits remove diffuse scattering, background level partly removed with conic pipes on 2d-detector.

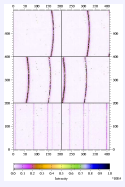

Raw images with Bragg lines, low and high angles.

Powder diffraction application (2)

Reconstructed Debye-Scherrer film or powder pattern

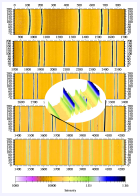

Resulting counts Y on pixel p :

$$Y_p = N_p^{-1} \Sigma f_q\, y_{q,i}$$

$y_{q,i}$ counts on image i of pixel q,
f_q flatfield of pixel q :

Film : $q \in Image_i \rightarrow p \in Image_{merged} : q = q(p,i)$

Minimisation : $\sum_q (Y_p - N_p^{-1} \sum_q f_q\, y_{q,i})^2$

Powder lines : $Y_{pcRing} \rightarrow Y_{Ring}$

$$\sum_{Ring} (Y_{Ring} - N_{Ring}^{-1} \sum_{pcRing} \sum_q f_q\, y_{q,i})^2$$

Powder diffraction application (3)

Reconstructed powder pattern — flatfield extraction

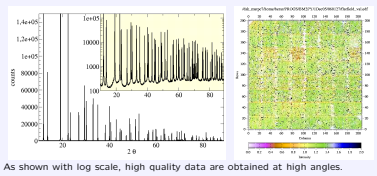

As shown with log scale, high quality data are obtained at high angles. Last detector assembly exhibit a quite uniform flatfield at 20 keV, even if pixels have not be very accutly tuned.

Kinetics potentiality of XPAD2

Whole electronic designed to allow kinetics studies (ms range)

- chips register 16bits + overflow
- on-board memories 32 bits
- exposure time : $1ms \rightarrow 8300s$
- dead time for reading :
  - whole image $2ms$
  - overflow $16\mu s$ each $10ms$
- on-board storage :
  - 423 images < $10ms$
  - 233 images >= $10ms$

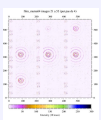

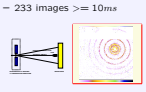

Images of 10 ms each taken of a 2s movies showing diffraction while the sample crosses the beam at D2AM SAXS camera.

Kinetics of quench studied by diffraction

Data collection is limited by the cell aperture, which has been designed for linear detector, a few frames of 20ms around crystallisation shown at 10 frames/s.

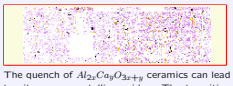

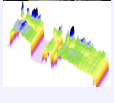

The quench of $Al_{2x}Ca_yO_{3x+y}$ ceramics can lead to vitrous or crystalline oxides. The transition between the liquid state and the cristalline one occurs in less than 20ms and may exhibit some transient phases.

Multilayers

Epitaxialy grown multilayer are now common samples to characterize : they need mapping of the reciprocal space which is time consuming. At the time such maps are recorded with slits and fixed (h, k, l) point of the reciprocal lattice, attenuators are often required near the substrate.

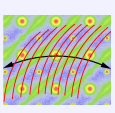

2-D detection allows an important improvement in these acquisitions but it needs to be able to manage high dynamics and to transform your reciprocal slices or volumes into reciprocal maps.

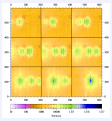

Multilayers : Ferroelectric superlattice

27 (17 PbTiO3,17 BaTiO3) superlattice / MgO :
large lattice mismatch → in-plane polarization → tetragonal distortion.
Physical behaviour of such compounds is primarily dependent on their epitaxial crystalline quality, their composition and their structural perfection.

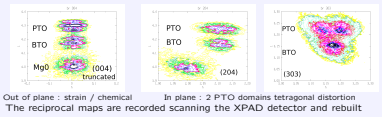

Out of plane : strain / chemical — In plane : 2 PTO domains tetragonal distortion

The reciprocal maps are recorded scanning the XPAD detector and rebuilt from the collected reciprocal slices. Compared to standard data collection the time can be reduced by 100. Intensity on substrate peak can reach $10^9 \nu/s$!

F. Lemarrec, E. Dooryhee and coll., IUCr (2005) Florence, Italy

from XPAD2 to XPAD3

- Obsolescence of the AMS-CMOS $0.8\,\mu m$ technology used for XPAD2
- A new XPAD3 using $0.25\,\mu m$ technology with $25\,\mu m$ bumps

	XPAD2	XPAD3	comments
polarization	both	e^+	2 chips : Si, CdTe
pixel size	$330\,\mu m$	$130\,\mu m$	
chip size	$8 \times 10\,mm^2$	$10 \times 15 mm^2$	→ reduce tiling
counting rate	$2.10^6 ph/s$	$2.10^5 ph/s$	≡ count/surface
energy range	(5) $15 \rightarrow 25 keV$	$7 \rightarrow 25 keV$	new analog chain
pixels/chip	$24 \times 25 = 600$	$80 \times 120 \approx 1.10^4$	
pixels/module	$8 \times 600 \approx 5.10^3$	$\approx 1.10^5$	
pixels/detector	$\approx 4.10^4$	$\approx 5.10^5$	
geometries	8×8 or 2×5	7×8 and ?	

- Chip design has been carried out
- Prototype is expected for mid 2006.